

Insight into substituent effects in Cal-B catalyzed transesterification by combining experimental and theoretical approaches

Zhong Ni · Xianfu Lin

Received: 17 May 2012 / Accepted: 25 July 2012 / Published online: 25 August 2012
© Springer-Verlag 2012

Abstract *Candida antarctica* lipase B (Cal-B) is one of the most recognized biocatalysts because of its high degree of selectivity in a broad range of synthetic applications of industrial importance. Herein, the substituent effects involved in transesterification catalyzed by Cal-B are explored in detail using a combination of experimental analysis and theoretical modeling. The transesterification ability of Cal-B was experimentally determined with 22 vinyl ester analogs and ribavirin as substrates and, on this basis, a series of quantitative structure-activity relationship (QSAR) models are developed using various structural parameters characterizing the variation in substituent groups of the substrate molecules. The resulting models exhibit a good stability and predictive power, from which five most important properties are highlighted and engaged to ascertain the structural basis and reaction mechanism underlying the transesterification. From the modeling analysis it is seen that the size, geometry, and charge distributions of substrate exert a significant effect on reaction yield, where, the size of the substituent group was the most significant impact factor on the reaction yield, the charge distribution was the second, and then the topological structure of the substrate.

Keywords *Candida antarctica* lipase B · Quantitative structure-activity relationship · Substituent effect · Transesterification

Electronic supplementary material The online version of this article (doi:10.1007/s00894-012-1552-7) contains supplementary material, which is available to authorized users.

Z. Ni
Institute of Life Sciences, Jiangsu University,
Zhenjiang 212013, People's Republic of China

X. Lin (✉)
Department of Chemistry, Zhejiang University,
Hangzhou 310027, People's Republic of China
e-mail: llc123@zju.edu.cn

Introduction

Enzyme, as a kind of excellent catalysts, attracted more and more interest from both the industrial and scientific communities, due to its good performance in the selective catalysis [1–6]. However, the detailed information involved in reaction mechanism mediated by diverse enzymes is still absent, which largely limits enzymatic applications in organic synthesis area. Although there were a variety of computational methods that have been developed aiming to shed light on the molecular mechanism of enzyme catalytic reaction based on enzyme's three-dimensional (3D) structures, for example, the docking technique which could predict the potential binding pose of small ligands within the active pocket of protein receptors and hence is employed to explain the reaction profile of substrate imposed by enzyme [7, 8], the obtained results are still suspicious if considering only the initial binding modes, but not reaction transition states, could be revealed [9]. Molecular dynamics (MD) is considered as one of the most important tools for understanding the physical basis of the structure and function of biological macromolecules [10, 11], but several drawbacks impair its applications in exploring enzymatic catalysis, such as limited sampling space, low frequency motions, and geometry rearrangements [12, 13]. On the other hand, the quantum mechanics/molecular mechanics (QM/MM)-mixed scheme has been successfully employed to dissect the reaction route of enzyme–substrate interactions, since the QM part takes directly into consideration the electronic structure of a molecule and therefore allows access to capture the chemical route of the reaction [14–16]. In our previous works, the QM/MM approach was successfully employed to evaluate the binding energies of enzyme–substrate complexes and predicate the stereoselectivity of *B.sub* lipase A toward the ketoprofen vinyl ester [17, 18]. Even so, some theoretical issues still exist in the QM/MM, especially those related to the description of the boundary between the QM and MM regions [19]. In addition,

the QM/MM is computationally expensive so that it can only be used to analyze a quite limited number of enzyme–substrate systems.

In the past several decades, the quantitative structure–activity relationship (QSAR) have been widely used in the drug design community to correlate the structural properties and biological activities of molecular agents from the statistical point of view [20, 21], which also represents a new and powerful approach to explore the reaction behavior catalyzed by enzyme [22]. Recently, several groups have successfully employed the QSAR methodology to examine the influence of structure varying on enzymatic activity and selectivity. For example, the detailed structural information of cyclooxygenase I and II activated by the dietary bioflavonoids was successfully elucidated under the assistance of the QSAR methodology [23]. Also, the enantioselectivity of Cal-B toward the alcohols with different substituent group was quantitative predicted with the aid of QSAR and a reliable result was obtained [24]. In addition, QSAR was employed to uncover the mechanism of protease and moreover differentiate the differences in mechanisms between serine and cysteine proteases [25].

Candida antarctic lipase B (CALB) is a widely used biocatalyst, due to its broad substrate specificity toward esters of primary and secondary alcohols, high stereoselectivity, high activity, and high thermostability [26–30]. In the present study, a series of vinyl esters analogs (substrate 2) with different substituent groups were synthesized under the catalysis of mercuric acetate. The yield of transesterification mediated by the *Candida antarctic* lipase B (Cal-B) was monitored by the HPLC, and the corresponding products were identified by NMR or/and MS. Subsequently, thousands of structural descriptors encoding the topological and physicochemical information of substrate molecules were generated and then correlated linearly with experimentally determined yields corresponding to these molecules, followed by a systematic validation to confirm the reliability of the built models which will be further used to investigate the substituent effects in the Cal-B catalyzed transesterification. We also give a systematic analysis on the stability and predictive power of the models in order to discuss the effectiveness and feasibility of QSAR strategy in guiding computer-aided substrate design (CASD).

Materials and methods

Experimental details

Materials

An immobilized lipase from *Candida antarctica* on macroporous acrylic resin (CALB) was purchased from Sigma

(USA). Ribavirin was obtained from commercial suppliers. Solvents for column chromatography were distilled before use.

Synthesis of the derivatives of vinyl esters

A series of vinyl ester with different chains were synthesized and determined. In a typical procedure, the reaction was initiated by adding 90 mg CAL-B to 30 ml acetone containing 0.36 g (1.5 mmol) ribavirin, 6 mmol vinyl fatty acid esters with different side chains respectively. The suspension was kept at 50 °C and shaken at 200 rpm. The reaction was terminated by filtering off the enzyme, and the filtrate was concentrated under reduced pressure. Formation of ribavirin ester was confirmed by TLC. The products were separated by silica gel column chromatography with an eluent consisting of ethyl acetate/methanol/water (17:3:1, by vol). The identities of the products were determined by ¹H NMR and ¹³C NMR spectra. Enzymatic synthesis of vinyl ribavirin fatty acid esters were shown in [Supporting information](#).

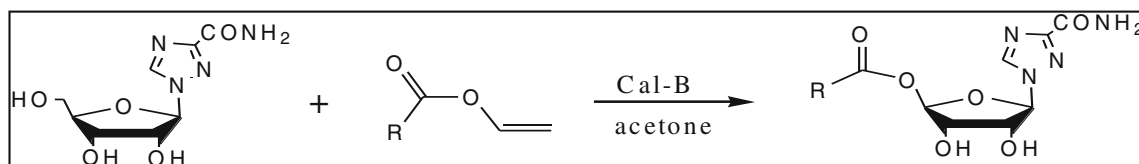
Enzymatic synthesis of ribavirin ester by transesterification

In a typical procedure, the reaction was initiated by adding 10 mg CALB to 3 ml acetone containing 36 mg (0.15 mmol) ribavirin, 0.6 mmol corresponding vinyl esters (synthesized) respectively. The suspension was kept at 50 °C and shaken at 200 rpm. The reaction was terminated by filtering off the enzyme, and the filtrate was concentrated under reduced pressure. Formation of ribavirin ester was confirmed by TLC. The products were separated by silica gel column chromatography with an eluent consisting of ethyl acetate/methanol/water (17:3:1, by vol). The identities of the products were determined by ¹H NMR and ¹³C NMR spectra, and the yields were conformed by the HPLC (SHIMADZU JAPAN).

Theoretical analysis

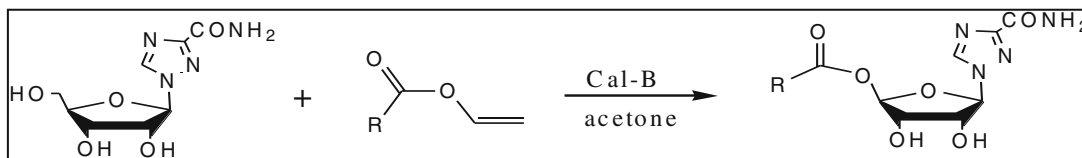
The substrate vinyl ester characterization

The calculation procedure of the vinyl esters descriptors is described as follows: the molecular structures of the 22 members were manually constructed using HyperChem 7.0 and optimized by energy-minimization in the level of AM1, finally saved in MOL format, then the output files of HyperChem were transferred into the CODESSA 2.7 [31, 32] to calculate five types of molecular descriptors [33] as constitutional (number of various types of atoms and bonds, number of rings, molecular weight, etc.), topological (Wiener index, Randic index, Kier-Hall shape index, etc.), geometrical (moments of inertia, molecular volume, molecular surface area, etc.), electrostatic (minimum and maximum

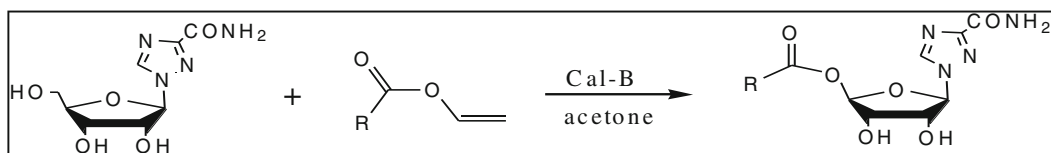
Table 1 The vinyl esters with different acid groups catalyzed by the CalB in acetone

Compound	R	Yield (%)		
		Expl ^e	Pred	Δ (Pred.-Expl.)
1		67	60.9	-6.1
2		93	70.1	-22.9
3		61	64.4	3.4
4		41	58.8	17.8

Table 1 (continued)

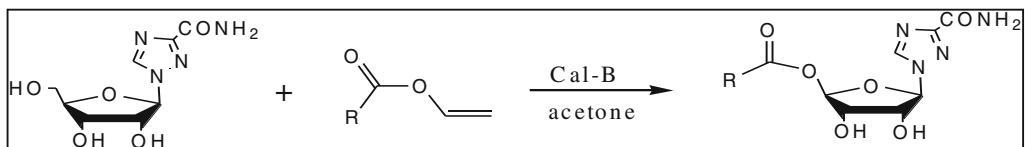


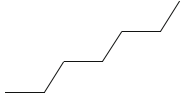
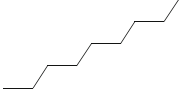
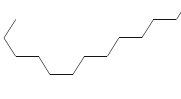
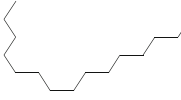
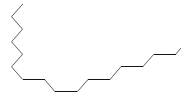
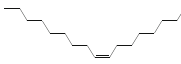
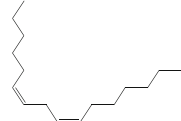
Compound	R	Yield (%)			
		Expl ^e	Pred	Δ	-Expl.)
5		22	37.4	15.4	
6		41	34.9	-6.2	
7		30	37.2	7.2	
8		26	31.2	5.2	
9		45	40.4	-4.6	

Table 1 (continued)

Compound	R	Yield (%)		
		Expe	Pred	^A (Pred.-Expe.)
10		41	36.7	-4.3
11		48	48.4	0.4
12		65	66.7	1.7
13		54	50.1	-3.9
14		55	48.1	-6.9
15		65	60.6	-4.4

Table 1 (continued)



Compound	R	Yield (%)		
		Expe	Pred	^Δ (Pred.-Expe.)
16		68	73.3	5.3
17		64	72.7	8.7
18		62	55.0	-7.0
19		28	33.8	5.8
20		20	21.7	1.7
21		31	38.0	7.0
22		32	16.9	-15.1

partial charges, polarity parameter, charged partial surface area descriptors, etc.), and thermodynamic descriptors (heat of formation, log P, molar refractivity, etc.). After the calculation of descriptors, the heuristic method implemented in CODESSA was used to select the significant descriptors. The statistical criteria considered for the selection of the best model were correlation coefficient (R^2), leave-one-out cross-validated correlation coefficient (R^2_{cv}), and Fisher criteria (F).

Results and discussion

Experimental results

The corresponding yields of the transesterification mediated by the CAL-B were obtained and shown in Table 1, as can be seen the substituted groups played an important role in governing the reactivity of substrates. When the substrates were substituted with the saturated alkyl chain (15–22), the yield decreased as the length of the chain increased. Substrates 15–18 all provided more than 60 % in yield, which was higher than substrates 19–22 obviously. However, the

influence of the chain length on the reaction was little, when the alkyl chain contains a vinyl group. All the substrates gave similar yield (11–14). More complicated results were obtained from the substrates with heterocyclics which linked the end of the alkyl chain (5–10). The results showed that the substrates that contained hydrophobic showed higher activity than those that contain hydrophilic (5, 6, 9 and 10). However, more than 26 % in yield was observed for the reactants without substituted group on the six-member ring. The results obtained from the substrates bearing five-member ring heterocyclics exhibited that shorter alkyl linker led to lower yield(1–4).

Heuristic MLR modeling

Using the approach described previously the first five of the best descriptors were collected (Table 2) and an optimal multi-linear relationship was developed based on the 22 analogs of the substrate (Eq. 1). Figure 1 is the plot of the predicted against experimental yield values for 22 analogs of the substrate, from which it can be seen that most samples are uniformly distributed along a fitting line with $r^2=0.74$.

$$\begin{aligned} \text{Yield}(\%) = & (501.3 \pm 66.45) - (454.3 \pm 81.1)\text{YZ Shadow/YZRectangle} \\ & - (12.1 \pm 2.298)\text{PPSA} - 3 - (9461.4 \pm 2310.8)\text{I}_c - (9.472 \pm 4.035)\text{ACIC}(\text{order } 2) \\ & - (426.3 \pm 223.22)\text{Max partial charge for a O atom} \end{aligned} \quad (1)$$

$N=22$, $R^2=0.78$, $F=11.76$, $s^2=108.1$, $R^2_{cv}=0.53$, where R^2 , the coefficient of determination, is a measure of the fitting ability of the regression model. Accordingly, it represents the variation involved in the observed (experimental) data that can be explained by regression model; the R^2 value closer to 1.0 indicates a better fitting of the model on training samples. The F -test reflects the ratio of the variance explained by the model and the variance due to the error in the model. High values of the F -test indicate that the model is statistically significant. The standard error is measured by the error mean square, s^2 , which expresses the variation of the residuals or the variation about the regression line. Thus the standard error measures the model error. N is the number of samples contained in whole data set.

The constitution of the regression equation includes two geometrical descriptors (YZ shadow/YZ rectangle and moment of inertia C), two electrostatic descriptors (PPSA-3 and max partial charge for O atom), and one topological descriptor (average complementary information content). These descriptors can be arranged based on their level of significance (“ t -criterion”) in the following order: “YZ shadow/YZ rectangle” > “PPSA-3

atomic charge weighted PPSA [Zefirov’s PC]” > “moment of inertia C” > “average complementary information content (order 2)” > “max partial charge for a O atom [Zefirov’s PC]”. It is worth nothing that all of the descriptors in Eq. 3 possess negative regression coefficients, indicating a reverse contribution of these structural properties to molecular self-assemble ability.

Table 2 Best five-descriptor QSAR model

ID	X	ΔX	t	Descriptor name
0	501.3	66.45	7.54	Intercept
1	-454.3	81.1	-5.602	YZ shadow/YZ rectangle
2	-12.1	2.298	-5.285	PPSA-3 atomic charge weighted PPSA [Zefirov’s PC]
3	-9461.4	2310.8	-4.094	Moment of inertia C
4	-9.472	4.035	-2.347	Average complementary information content (order 2)
5	-426.3	223.22	-1.91	Max partial charge for a O atom [Zefirov’s PC]

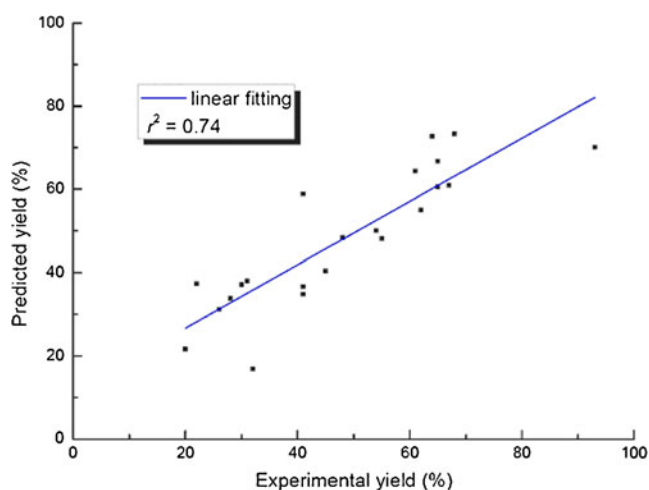


Fig. 1 Predicted vs. experimental yield of transesterification

The most significant descriptor in the above correlation is the YZ shadow/YZ rectangle, a shadow index, which is related to the size (natural shadow indices) and geometrical shape (normalized shadows indices) of the molecule. YZ shadow/YZ rectangle is the areas of the shadows S_2 of the molecule as projected on the YZ plane. The normalized areas are calculated as the ratios $S_2/(Y_{\max} Z_{\max})$, where Y_{\max} and Z_{\max} are the maximum dimensions of the molecule along the corresponding axes. The shadow areas are calculated by applying 2D square grid on the molecular projection and by summation of the areas of squares overlapped with a projection. The value of the YZ shadow/YZ rectangle increases with the size of the fragment, which causes a decrease in yield.

Moment of inertia C (I_C) is an another geometrical descriptor, it characterizes the mass distribution in the molecule and can be calculated as follows

$$I_C = \sum_i m_i r_{iz}^2, \quad (2)$$

where m_i is the atomic masses and r_{iz} denote the distance of the i th atomic nucleus from the main rotational axes Z of the molecule. It is related to the optimal size and shape of

the active molecules; molecules of size larger than the optimal may well experience steric hindrance and thus inability to bind efficiently to the target.

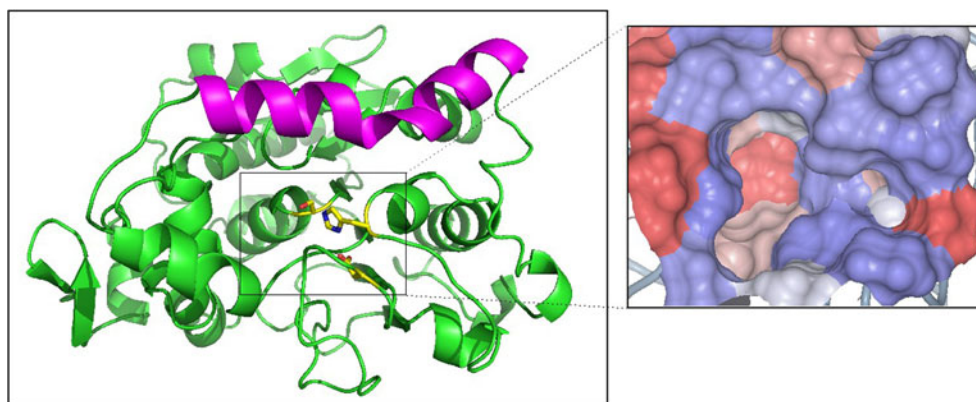
These reasons could be explained by that, basically, in the process of the enzymatic reaction, the formation of enzyme-substrate complex is crucial for the enzyme mediated reaction, and our previous works showed that the larger binding energy between enzyme-substrate complex, the faster the reaction [18]. In general, whether forming the effective enzyme-substrate complex would largely influence the reactions which were catalyzed by the enzymes, the effect of the size of substrate toward the enzymatic reaction is remarkable. In this study, the chemical properties of the substrates (ID 15–22) are similar, except the chain length of the substituted groups. The experimental results showed that the yields of the substrate 15–18 are over 60 %, but for the substrate (ID 19–22), the corresponding yields are about 30 %. The main difference in yield was attributed to the difference in size of the substituted group in substrate 2. The chain length of the substituted group (ID 15–18) is less than 13 carbon atoms, but for the 19–22, the related chain length is larger than 15 carbon atoms. These results indicated that the size of the substrate largely affect the reaction catalyzed by the CALB. Thus, YZ Shadow/YZ Rectangle and the Moment of inertia C have negative relations with the yield of the reaction.

PPSA-3, is a charged partial surface area descriptor which combines information on the atomic contributions to the solvent-accessible surface area of the molecule with partial atomic charge information. PPSA-3 is defined as the following formula (3):

$$\text{PPSA} - 3 = \sum (+SA_i)(Q_j^+), \quad (3)$$

where $+SA_i$ is the surface area contributions of the i th positive in the molecule. Q_j^+ is the partial atomic charges for the i th positive atoms.

Fig. 2 The structure of the *Candida antarctica* lipase A and the hydrophobic pocket of the active site. The catalytic residues were shown in stick mode; the active site colored blue represent hydrophobic areas and red represents hydrophilic areas



The electrostatic catapult model, proposed by Peteren [34], described the release of the products mediated by the enzyme. The larger the value of the PPSA-3, the more positive charges in the substrate, lead to the efficiency decrease in transesterification catalyzed by the Cal-B. Because the electrostatic interaction between the small molecules with positive charges and the catalytic cleft of lipase with negative charges [35] might hinder the release of the products.

Max partial charge for an O atom [Zefirov's PC] is the electrostatic descriptor that reflects characteristics of the charge distribution of the molecule, the partial charges in the molecule can be calculated using the approach proposed either by Zefirov [36], which takes molecular electronegativity as a geometric mean of atomic electronegativities, or by the widely used Gasteiger-Marsili method, which involves iterative partial equalization of orbital electronegativity [37]. In this study, this descriptor reflected the partial charge for O atom of the ester carbonyl group of the substrate, in the process of the reaction catalyzed by the lipase, this O atom acts as the acceptor, form the hydrogen bond with the hydrogen-bonding donors which were called oxyanion hole in lipase [38]. Obviously, too strong a hydrogen bond might influence the subsequent steps of the catalytic process mediated by the Cal-B, and thus reduce the reaction efficiency.

Average Complementary Information content (order 2) (ACIC) is a topological descriptor which describe the atomic connectivity in the molecule, and calculated as follows

$${}^k\overline{CIC} = \log_2 n - {}^k\overline{IC}, \quad (4)$$

where \overline{IC} is the average information content defined on the basis of the Shannon information theory, n is a total number of atoms in the molecule, k is the number of atomic layers in the coordination sphere around a given atom that are accounted for, and q donates the number of edges in the molecular graph. They express the bonding properties and structural properties in the molecule which related to the number of atoms as well as the number of atomic layers.

In the process of the forming enzyme-substrate complex, there are some complementary non-bonding interactions in the process of the approach between enzymes and substrates, such as steric, electrostatic and hydrophobic factors and so on. According to the lock-key theory or induced-fit theory, shape fitting is one of the most important forces to drive enzyme and substrate to form the complex. If the substrates have a complement shape to the active site of enzyme, that will not only facilitate the binding but also promote the reaction mediated by the enzyme. This result is also consistent with the experimental data which shows that appropriate length of the hydrophobic chain of the substrate

facilitates the reaction mediated by the Cal-B and the hydrophobic property for active site of Cal-B (Fig. 2). Thus this topological descriptor showed negative relations with the yield of the reaction.

In general, the matching between enzyme and substrate is very important for the enzymatic reaction. It is said that the substrate would be the part of the enzyme after the formation of enzyme-substrate complex. The subsequent changes in the conformation of the complex macromolecule would ultimately launch the catalytic process by itself. Obviously, the intermolecular interactions dynamically involved in catalysis are that the energetics of the reaction can be easily manipulated to produce catalysis. So the better fit of the substrate-enzyme complex, the greater contribution to the decrease of active energy barrier.

Conclusions

In this presentation, a series of vinyl esters with different substituted groups were synthesised, then act as substrates process transesterification with the ribavirin catalyzed by the Cal-B, and the products were verified by the IR, ^1H NMR, ^{13}C NMR spectra and MS. The experiment results showed that the conversions of the reactions catalyzed by the *Candida antarctic* lipase B were largely influenced by the substituted group of the vinyl esters.

In addition, there is a strong correlation between predictive and experimental yield of reaction mediated by the *Candida antarctic* lipase B with significant correlation coefficient $r=0.74$.

The QSAR results elucidate that the size, charge distribution and the geometry of substrate 2 affects the reaction yield which is mediated by the *Candida antarctic* lipase B, R^2 and R_{cv}^2 of the QSAR model are 0.78 and 0.53, respectively. The results show that the QSAR model is robust and has a considerable predictive ability.

Acknowledgments This work was supported by the National Basic Research Program of China (973 Program, No 2011CBA00801 and 2009CB724700).

References

- Acetti D, Brenna E, Fuganti C, Gatti FG, Serra S (2009) Enzyme-catalysed approach to the preparation of triazole antifungals: synthesis of (-)-genaconazole. *Tetrahedron-Asymmetry* 20:2413–2420
- Alatorre-Santamaria S, Gotor-Fernandez V, Gotor V (2009) Stereoselective chemoenzymatic synthesis of enantiopure 1-(Heteroaryl)ethanamines by lipase-catalysed kinetic resolutions. *Eur J Org Chem* 15:2533–2538

3. Asikainen M, Krause N (2009) Tandem enzyme/gold-catalysis: from racemic alpha-allenic acetates to enantiomerically enriched 2,5-dihydrofurans in one pot. *Adv Synth Catal* 351:2305–2309
4. Banoth L, Singh M, Tekewe A, Banerjee U (2009) Increased enantioselectivity of lipase in the transesterification of dl-(+/-)-3-phenyllactic acid in ionic liquids. *Biocatal Biotransfor* 27:263–270
5. Reetz MT, Wu S (2009) Laboratory evolution of robust and enantioselective Baeyer-Villiger monooxygenases for asymmetric catalysis. *J Am Chem Soc* 131:15424–15432
6. Reetz MT (2002) Lipases as practical biocatalysts. *Curr Opin Chem Biol* 6:145–150
7. Yelekci K, Karahan O, Toprakci M (2007) Docking of novel reversible monoamine oxidase-B inhibitors: efficient prediction of ligand binding sites and estimation of inhibitors thermodynamic properties. *J Neural Transm* 114:725–732
8. Sotriffer CA, Flader W, Winger RH, Rode BM, Liedl KR, Varga JM (2000) Automated docking of ligands to antibodies: methods and applications. *Methods* 20:280–291
9. Pujadas G, Vaque M, Ardevol A, Blade C, Salvqado MJ, Blay M, Fernandez-Larrea J, Arola L (2008) Protein-ligand docking: a review of recent advances and future perspectives. *Curr Pharm Anal* 4:1–19
10. Hess B, Kutzner C, Spoel DVD, Lindahl E (2008) GROMACS 4: algorithms for highly efficient, load-balanced, and scalable molecular simulation. *J Chem Theor Comput* 4:435–447
11. MacKerell AD, Banavali NK (2000) All-atom empirical force field for nucleic acids: II. Application to molecular dynamics simulations of DNA and RNA in solution. *J Comput Chem* 21:105–120
12. Karplus M, McCammon JA (2002) Molecular dynamics simulations of biomolecules. *Nat Struct Biol* 9:646–652
13. Allison JR, Bergeler M, Hansen N, van Gunsteren WF (2011) Current computer modeling cannot explain why two highly similar sequences fold into different structures. *Biochemistry* 50:10965–10973
14. Monard G, Merz KM (1999) Combined quantum mechanical/molecular mechanical methodologies applied to biomolecular systems. *Acc Chem Res* 32:904–911
15. Tian L, Friesner RA (2009) QM/MM simulation on P450 BM3 enzyme catalysis mechanism. *J Chem Theor Comput* 5:1421–1431
16. Szeto MWY, Mujika JL, Zurek J, Muholland AJ, Harvey JN (2009) QM/MM study on the mechanism of peptide hydrolysis by carboxypeptidase A. *J Mol Struct (THEOCHEM)* 898:106–114
17. Ni Z, Jin X, Zhou P, Wu Q, Lin XF (2011) A combination of computational and experimental approaches to investigate the binding behavior of B.sub lipase a mutants with substrate pNPP. *Mol Inf* 30:359–367
18. Ni Z, Zhou P, Jin X, Lin XF (2011) Integrating in silico and in vitro approaches to dissect the stereoselectivity of Bacillus subtilis lipase a toward Ketoprofen Vinyl Ester. *Chem Biol Drug Des* 78:301–308
19. Moro G, Vonati L, Bruschi M, Cosentino U, Gioia LD, Fantucci PC, Pandini A, Papaleo E, Pitea D, Saracino GAA (2007) Computational approaches to shed light on molecular mechanisms in biological processes. *Theo Chem Acc* 117:723–741
20. Bello JF, Llama EF, del Campo C, Cabezas MJ, Sinisterra JV (1993) Structure activity relationship relationship in the hydrolysis of N-benzoylphenylalanine esters catalyzed by alpha-chymotrypsin. *J Mol Catal* 78:91–112
21. Debnath AK (2005) Application of 3D-QSAR techniques in anti-HIV-1 drug design—an overview. *Curr Pharm Des* 11:3091–3110
22. Brown N, Lewis RA (2006) Exploiting QSAR methods in lead optimization. *Curr Opin Drug Disc* 9:419–424
23. Wang P, Bai HW, Zhu BT (2010) Structural basis for certain naturally occurring bioflavonoids to function as reducing co-substrates of Cyclooxygenase I and II. *PLoS One* 5: e12316
24. Gu J, Liu J, Yu H (2011) Quantitative prediction of enantioselectivity of Candida antarctica lipase B by combining docking simulations and quantitative structure–activity relationship (QSAR) analysis. *J Mol Catal B Enzym* 72:238–247
25. Shokhen M, Traube T, Vijayakumar S, Hirsch M, Uritsky N, Albeck A (2011) Differentiating serine and cysteine protease mechanisms by new covalent QSAR descriptors. *Chem Bio Chem* 12:1023–1026
26. Juhl PB, Doderer K, Hollmann F, Thum O, Pleiss J (2010) Engineering of Candida antarctica lipase B for hydrolysis of bulky carboxylic acid esters. *J Biotechnol* 150:474–480
27. Zhang YH, Xu CF, Li JF, Yuan CY (2003) Enzymatic synthesis of optically active delta-hydroxy-beta-ketoalkanephosphonates. *Tetrahedron Asymmetr* 14:63–70
28. Vieira TO, Ferraz MCF, Andrade LH, Porto ALM (2006) Highly enantioselective enzymatic resolution of cis-fused octalols mediated by Candida antarctica lipase (Novozym 435). *Tetrahedron Asymmetr* 17:1990–1994
29. Zhang NY, Suen WC, Windsor W, Xiao L, Madison V, Zaks A (2003) Improving tolerance of Candida antarctica lipase B towards irreversible thermal inactivation through directed evolution. *Protein Eng* 16:599–605
30. Hernandez K, Fernandez-Lafuente R (2011) Lipase B from Candida antarctica immobilized on octadecyl Sepabeads: a very stable biocatalyst in the presence of hydrogen peroxide. *Process Biochem* 46:873–878
31. Katritzky AR, Lgnatchenko ES, Barcock RA, Lobanov VS, Karelson M (1994) Prediction of gas-chromatographic retention times and response factors using a general quantitative structure–property relationship treatment. *Anal Chem* 66:1799–1807
32. Ivanciuc O (1997) CODESSA version 2.13 for windows. *J Chem Inf Comput Sci* 37:405–406
33. Karelson M, Maran U, Wang YL, Katritzky AR (1999) QSPR and QSAR models derived using large molecular descriptor spaces. A review of CODESSA applications. *Collect Czech Chem C* 64:1551–1571
34. Neves-Petersen MT, Petersen EL, Fojan P, Noronha M, Madsen RG, Petersen SB (2001) Engineering the pH-optimum of a triglyceride lipase: from predictions based on electrostatic computations to experimental results. *J Biotechnol* 87:225–254
35. Petersen MTN, Fojan P, Petersen SB (2001) How do lipases and esterases work: the electrostatic contribution. *J Biotechnol* 85:115–147
36. Zefirov NS, Palyulin VA (2002) Fragmental approach in QSPR. *J Chem Inf Comput Sci* 42:1112–1122
37. Gasteiger J, Marsili M (1980) Iterative partial equalization of orbital electronegativity—a rapid access to atomic charges. *Tetrahedron* 36:3219–3228
38. Schrag JD, Li YG, Wu S, Cygler M (1991) Ser-His-Glu triad forms the catalytic site of the lipase from geotrichum-candidadum. *Nature* 351:761–764